Journal of Ambient Intelligence and Humanized Computing
https://doi.org/10.1007/s12652-021-03681-0

ORIGINAL RESEARCH

MRI de-noising using improved unbiased NLM filter

S. Sahu[1] · A. Anand[2] · A. K. Singh[3] · A. K. Agrawal[4] · M. P. Singh[3]

Received: 16 July 2021 / Accepted: 15 December 2021

Abstract
The magnetic resonance images focus on soft tissues, and it is often necessary for healthcare professionals to reach the final conclusion in clinical diagnosis. However, these images are often affected by random noise, which decreases the visual quality and reliability of the images. This paper presents an improved unbiased non-local mean (NLM) filter to solve the de-noising issue in the MRI images. Local statistics of the noise is combined with the NLM filter to design an unbiased NLM filter. First of all, the Gaussian noise information is extracted from the noisy image by performing the wavelet decomposition, statistically modeling the diagonal sub-band wavelet coefficients, and estimating the noise variance by applying the median absolute deviation (MAD) estimator. Next, the Rician noise is removed by applying a NLM filter which averages the noisy pixels by a Gaussian weight factor. Finally, the NLM filtered output pixels are unbiased by applying the noise bias subtraction method for recovering the original pixel values. Our experiments on real MRI and synthetic images demonstrate that promising results that can be obtained much superior than results estimated using existing non-local mean filtering schemes.

Keywords MRI image · Non-local mean (NLM) filter · MAD estimator · Wavelet decomposition

1 Introduction

Magnetic resonance imaging (MRI) is a medical image modality employed in health care system that provides images of internal tissues and organs in the subject body for demonstrating the physiological or pathological anomalies (Heo et al. 2020). Medical image processing plays an important role in healthcare sector. Noise may result inaccurate diagnosis which leads to loss of human life. This motivates to develop a methodology that removes the noise and results accurate diagnosis. Now a day the MRI has widespread use in healthcare systems for biomedical research and diagnostic medicine but it also covers a broad area of applications in different sectors such as pharmaceutical applications (Richardson et al. 2005), forensic imaging, study of internal body structure of animal species, study of anatomy of plants and structure of fossils etc., as shown in Fig. 1.

MRI can capture 2D and 3D images and is a non-invasive and non-destructive in nature. MR imaging method has basically two functional blocks: acquisition and reconstruction. Following Fig. 2 shows the MR imaging process. The acquisition block acquires the RF signals from the subject's body, digitizes and stores the digitized data in K space (a memory configuration). The reconstruction block reconstructs the MR image from the acquired signal. The number of rows and columns (size) of the K space depends upon the image details requirements.

An important drawback of MR image is the limited acquisition time, made for patient's comfort that affects visual quality and results decrease in signal-to-noise ratio (SNR) (Hanchate and Joshi 2020a). MRI acquisition process results high Gaussian density noise and affects the disease diagnosis

✉ A. K. Singh
amit.singh@nitp.ac.in

S. Sahu
simahal@mrec.ac.in

A. Anand
ashima1795@gmail.com; ashima.anand@thapar.edu

A. K. Agrawal
agrawal.amrit4@gmail.com

M. P. Singh
mps@nitp.ac.in

1 Department of ECE, Malla Reddy Engineering College (Autonomous), Maisammaguda, Hyderabad, Telangana, India

2 Department of CSE, Thapar Institute of Engineering and Technology, Patiala, Punjab, India

3 Department of Computer Science and Engineering, NIT Patna, Patna, India

4 Department of CSE, Galgotias College of Engineering and Technology, Greater Noida, India

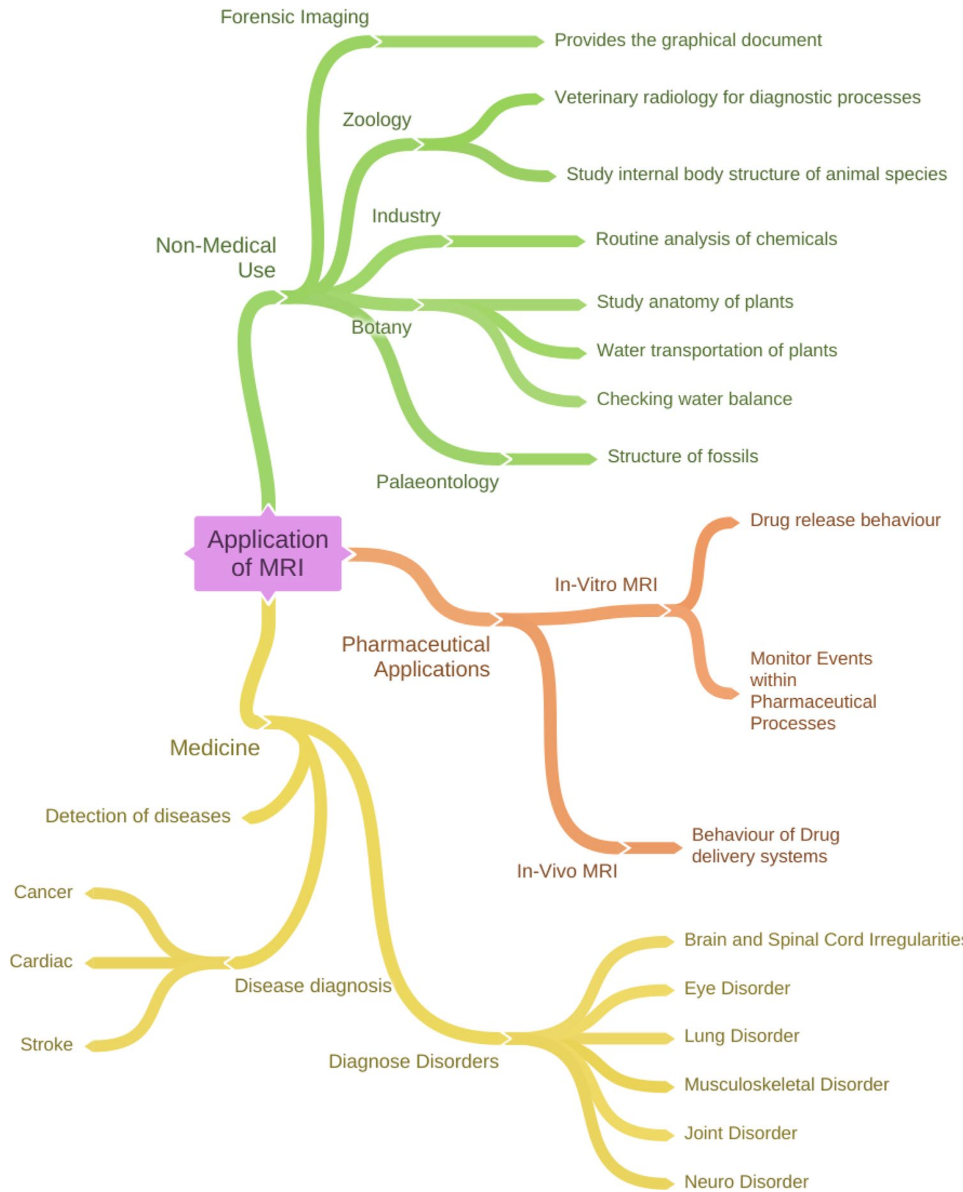

Fig. 1 Applications of MRI in different areas

and management process (Redpath 1998). The main reason of noise in MRI is artifacts during image acquisition and reconstruction process and results image degradation. One of the factors which degrades the MR images and also affect the quantitative measurements extracted from the image is the thermal noise (Zhu et al. 2009). During the reconstruction process of MR image, the main sources of artifacts are: magnetic susceptibility of scanned object, pulse sequence design, radio frequency coil and motions (rigid and non-rigid) (Macovski 1996). Based on the acquisition system, the random noise in MRI may be Rician or Gaussian noise. Single coil acquisition technique results Rician noise while parallel coil acquisition technique results Gaussian noise with zero mean (Sijbers et al. 1998). High SNR is highly required for true interpretation of MR image data (Kanoun et al. 2020) and this necessitates the de-noising of MR images.

An improved de-noising methodology is presented in this paper motivated by the work of Manjón et al. (2008) that utilizes the non-local features of the NLM method. A noise estimation method based on non-local mean was proposed by them for removing Gaussian and Rician noise from MRI. In our paper special attention is given for finding the accurate noise variance which Manjón et al. (2008) failed to explain.

In this paper, we develop a robust de-noising mechanism to recover MR images degraded by Gaussian and Rician noise. Here, multi-resolution approach is combined with the non-local mean (NLM) filter to design an unbiased NLM filter. The noise variance is calculated from the complex

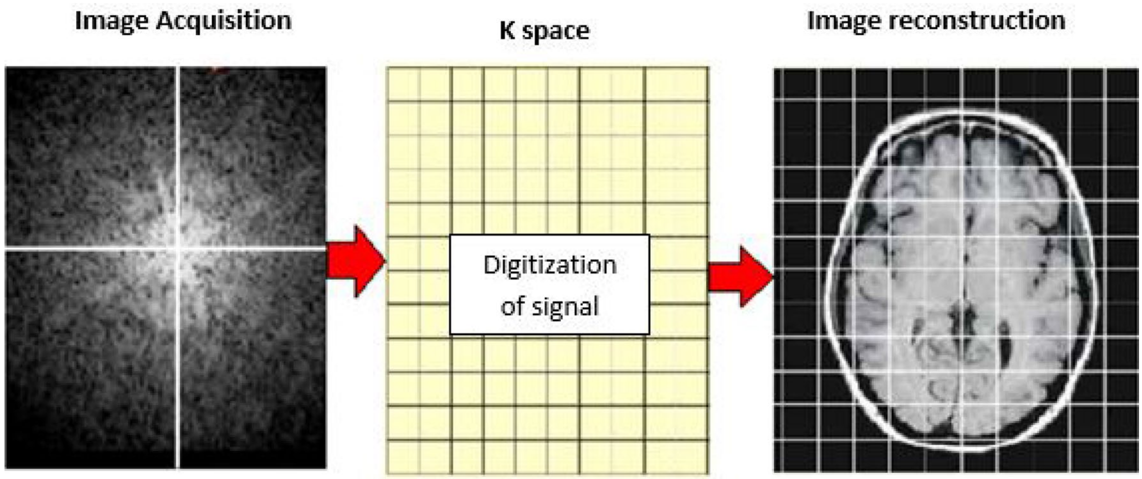

Fig. 2 MR imaging process

dataset assuming the noise is distributed in Gaussian nature. The simulated results demonstrate that the proposed mechanism performed more efficiently than the other traditional schemes. It indicates a considerable improvement of 25.32%, 11.26%, 19.93%, 28.31% and 30.81% in Peak Signal to Noise Ratio (PSNR), Correlation of coefficient (CoC), Pratt's Figure of Merit (FOM), Mean Structural Similarity Index (MSSIM), and Edge Preservation Index (EPI) performance parameters, respectively over the existing Unbiased NLM filters.

The rest of the paper is arranged like below. Section 2 includes the relevant works. Section 3 introduces our proposed filter for noisy MR images. Section 4 gives the experimental results and discussion, followed by the conclusions along with future scope in the Sect. 5.

2 Related work

To date, a variety of de-noising schemes for MRI images have been widely concerned by many scholars and researchers. Therefore, we review them separately. During MR image acquisition the most common approach to reduce the random noise is increasing the count of signal averages and speed is the main disadvantage of this method (Sahu et al. 2019c). This limitation can be overcome by applying algorithmic approached de-noising methods likely; filtering approached methods, transform based methods and statistical approached methods.

Filtering approached methods can be categorized as spatial, temporal, frequency-domain (McVeigh et al. 1985), NLM (Manjon et al. 2007), Bilateral (Hamarneh and Hradsky 2007) and anisotropic diffusion (Krissian and Aja-Fernández 2009). An MRI de-noising method was proposed by Hong et al. (2020) for Rician noise removal. The author developed a network called feature fusion and attention network (FFA-DMRI), which consists of three blocks namely feature block, fusion block and attention block for separating noise from MR data. A hybrid noise removal methodology for MRI was developed by Romdhane et al. (2021). Their approach was based on anisotropic diffusion filter and NLM filter. They validated the method on In-Vivo data. Xie et al. (2020) developed a machine learning based de-noising method for MRI image of low SNR. In NLM filtering method the image pixels of similar value are averaged based on their intensity distance. Based on this principle, bilateral filter is designed. The difference between these filters and NLM filter is that, NLM filter supports the comparison of regions than pixel comparison. The original NLM filter utilizes Euclidean distance for similarity measurement (Buades et al. 2005). Further this approach was improved by Rajan et al. (2014). They proposed KS distance for similarity measurement. He and Greenshields (2008) proposed a Non Local Maximum Likelihood Estimation (NLML) algorithm for de-noising MR image affected by Rician noise. They developed a non-local maximum likelihood estimator that estimates the level of redundancy in an MR image. An MRI de-noising technique was presented by Chen et al. (2020) which utilized the principle of NLM filter. They combined adaptive NLM filter with Fuzzy C-Means algorithm to remove Rician noise. An improved non local correction patch based de-noising technique was proposed by Sarkar et al. (2020), to de-noise brain MRI. Their proposed method was based on NLM filtering technique. The input image was divided into smooth component and periodic component by utilizing a Fast Fourier Transform (FFT) algorithm. Further non local based averaging was used to de-noise both the components. A de-noising algorithm based on Shearlet transform was developed by Sharma and

Chaurasia (2021). They designed a NLM filter by combining Shearlet filter and non-sub-sampled pyramid filter.

A non local (NL) based MRI de-noising method was proposed by Leal et al. (2020) for removing noise from MR image. Their method was based on sparse representation by using NL single value decomposition algorithm.

Transform based methods are preferred than the filtering approached methods commonly Wavelet transform due to its multiresolution and multiscale property. In transform based methods, the noisy image is converted to transform coefficients by applying mathematical based transforms such as Wavelet (Kagoiya and Mwangi 2017), contourlet (Anila et al. 2017) and Curvelet (Bhadauria and Dewal 2013) transforms. Further the transform coefficients are threshold and the image is recovered by applying inverse transformation method. A transform based gamma correction methodology was developed by Kollem et al. (2020) to de-noise brain MRI. In this method the noisy pixels were threshold by a generalized cross-validation method. Combining Wavelet transform and Laplace transform a de-noising method was proposed by Upadhyay et al. (2021) for removing noise from MR image. Hanchate and Joshi (2020b) developed a noise removal methodology by grouping Wavelet shrinkage and 3D Discrete Wavelet Transform (DWT) for de-noising MRI. The threshold value was decided by implementing a noise validation de-noising technique.

The transform based de-noising methods heavily depend upon the threshold value selection. A correct estimation of the threshold value is required to remove the noise effectively. This problem is solved by applying statistical models and estimators which utilizes the local statistics of the data distribution to find the threshold value (Sahu et al. 2020a). Das et al. (2020) presented de-noising methodology for removing noise and preserving edge and details of MR image. They utilized an estimator (local variance based) to estimate the noise and, statistical edge stopping function for image details preservation. A statistical based de-noising method was presented by Sahu et al. (2020b) for MR images. In this method wavelet coefficient data distribution was fitted to a Normal Inverse Gaussian (NIG) density function to extract the noise-free pixels and noise variance was estimated by MAD estimator.

The MR noise reduction algorithm based on NLM filter is an excellent methodology to remove noise and enhance the diagnostic accuracy due to its non-local self-similarity nature (Heo et al. 2020). In other filtering methods there is a chance of loss of inherent information which is minimized by applying the improved unbiased NLM filter that utilizes a MAD estimator for effective noise calculation and so preserves the edge and details information.

3 Proposed algorithm

In this section, we concentrate on the proposed model to recover MR images degraded by Gaussian and Rician noise. First of all, the Gaussian noise information is extracted from the noisy image by performing the wavelet decomposition, statistically modeling the diagonal sub-band wavelet coefficients, and estimating the noise variance by applying the MAD estimator. Next, the Rician noise is removed by applying a NLM filter which averages the noisy pixels by a Gaussian weight factor. Finally, the NLM filtered output pixels are unbiased by applying the noise bias subtraction method for recovering the original pixel values. Figure 3 presents the basic process of our de-noising scheme, and the details are as follows.

Step 1. Wavelet decomposition of the input image.

The wavelet decomposition of an image of size A × B number can be defined mathematically as Gonzalez and Woods (2002), Sahu et al. (2018, 2019a, b):

$$\begin{aligned} W(a,b) = & \frac{1}{\sqrt{AB}} \sum_{p=1}^{A} \sum_{q=1}^{B} f_M^A(p,q) \varphi_M^A(a,b,p,q) \\ & + \sum_{m=1}^{M} \sum_{N \epsilon H,V,D} \sum_{p=1}^{A} \sum_{q=1}^{B} f_m^N(p,q) \Psi_m^N(a,b,p,q) \end{aligned} \tag{1}$$

where $\varphi(.)$ and $\Psi(.)$ are scaling and wavelet functions respectively. $N\epsilon$ H,V,D represents horizontal, vertical and diagonal sub-bands respectively and a, b, p and q are the variables. f_M^A (p,q), φ_M^A (a,b,p,q), f_m^N (p,q), and Ψ_m^N (a,b,p,q) are M level approximation coefficients, 2D scaling coefficients, detailed coefficients and 2D wavelet coefficients respectively. The 2D scaling and wavelet functions are defined as follows:

$$\varphi_M^A(a,b,p,q) = 2^{\frac{M}{2}} \varphi\left(2^M a - p\right) \varphi\left(2^M b - q\right) \tag{2}$$

$$\Psi_M^H(a,b,p,q) = 2^{\frac{M}{2}} \psi\left(2^M a - p\right) \varphi\left(2^M b - q\right) \tag{3}$$

$$\Psi_M^V(a,b,p,q) = 2^{\frac{M}{2}} \varphi\left(2^M a - p\right) \psi\left(2^M b - q\right) \tag{4}$$

$$\Psi_M^D(a,b,p,q) = 2^{\frac{M}{2}} \psi\left(2^M a - p\right) \psi\left(2^M b - q\right) \tag{5}$$

Step 2. Noise variance estimation using the MAD Estimator.

An MAD estimator is applied in first level of diagonal detailed Sub-band (HH1) to find the variance of the Gaussian

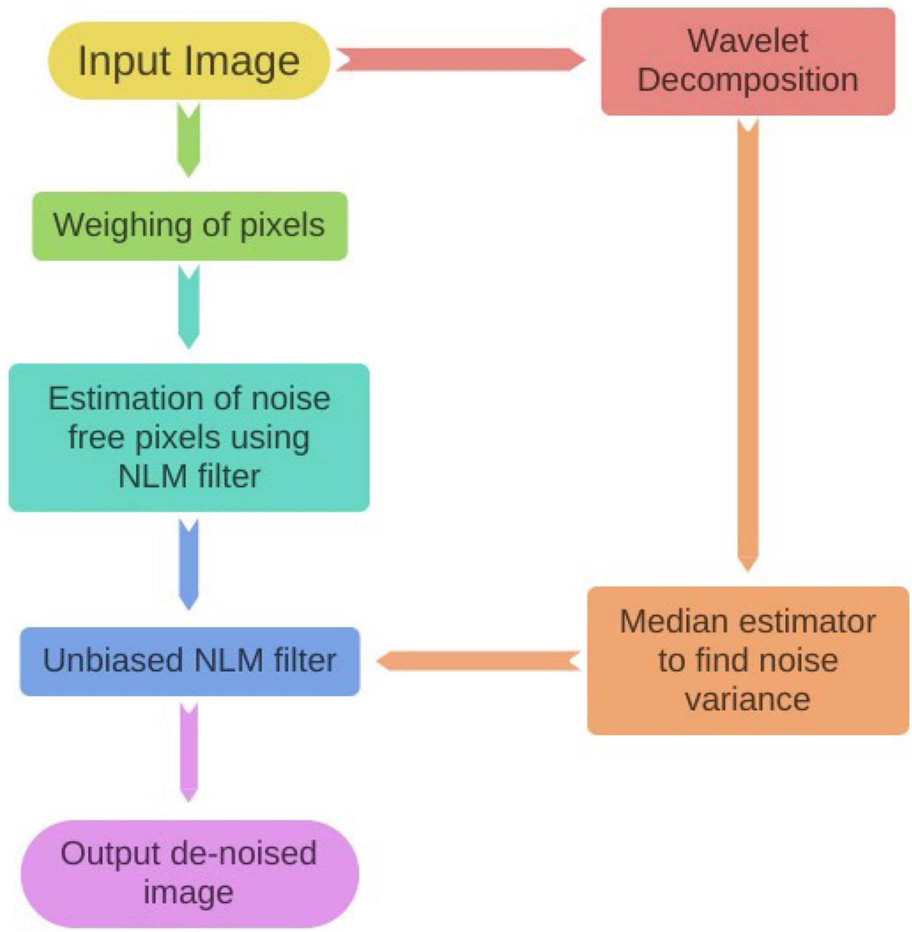

Fig. 3 Flow chart of proposed de-noising scheme

noise. The diagonal detailed sub-band contains most of the noise information. The noise variance σ_n^2 is given by:

$$\hat{\sigma}_\eta^2 = \left(\frac{median(|HH1|)}{0.6745}\right)^2 \tag{6}$$

The wavelet transform of the Gaussian noise is also Gaussian in nature. So a Normal PDF is used to model the diagonal detailed wavelet coefficients. The density distribution of wavelet coefficients of HH1 sub-band is shown in Fig. 4. The goodness-of-fit of HH1 sub-band with Normal PDF and CDF are shown in Figs. 5 and 6 respectively. It can be seen that the Gaussian PDF and CDF fits well with the HH1 sub-band data.

Step 3. Calculation of weighing coefficients.

Let W(c,d,a,b) be the weighing Coefficient where,

$$\sum_{a=0}^{A-1}\sum_{b=0}^{B-1} W(c,d,a,b) = 1.$$

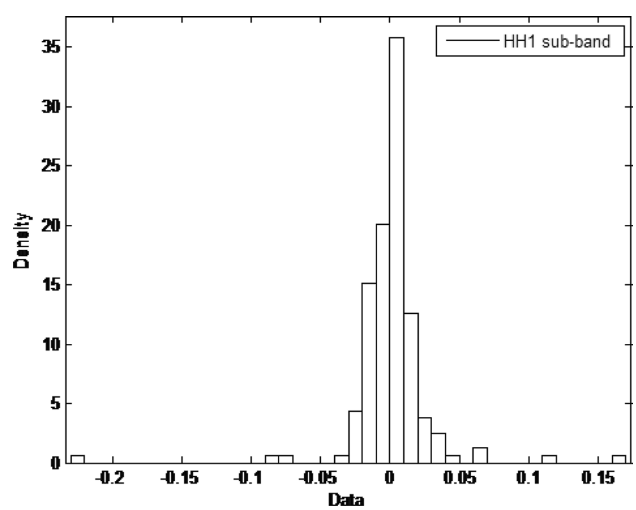

Fig. 4 Distribution of wavelet coefficients in HH1 sub-band for MR image

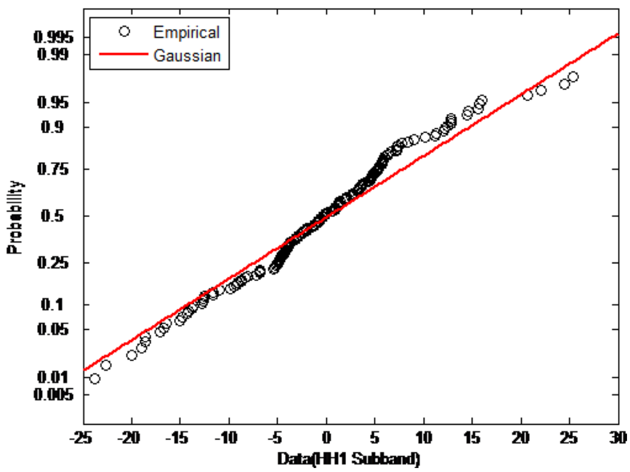

Fig. 5 Goodness-of-fit graph of HH1 sub-band: PDF plot

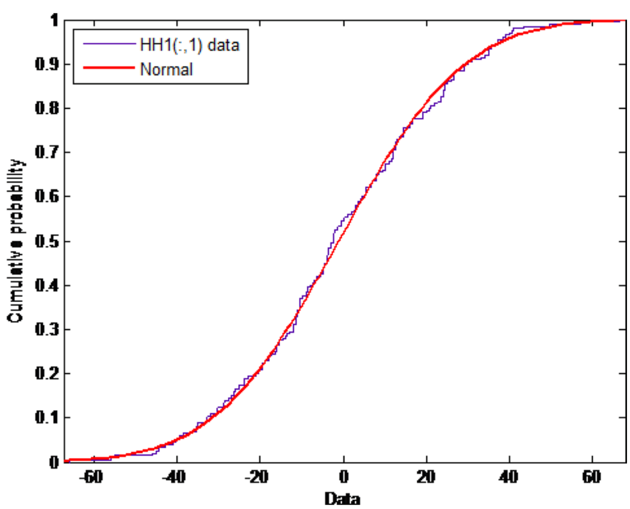

Fig. 6 Goodness of fit graph of HH1 sub-band: CDF plot

The weighing coefficient for the image of size A × B can be defined as:

$$W(c,d,a,b) = \frac{1}{Z(c,d)} e^{\frac{-G_\sigma ||g(N_{cd}) - g(N_{ab})||^2}{h^2}} \tag{7}$$

where c, d, b, and a are the variables and G_σ = Gaussian weighing function with unity standard deviation and zero mean. The parameter h is defined as smoothing parameter, set depending on the value of noise standard deviation and $\|\text{-}\|^2$ is the Euclidean distance (Gaussian weighted). Z(c,d) is the normalizing constant defined as:

$$Z(c,d) = \sum_{a=0}^{A-1} \sum_{b=0}^{B-1} e^{\frac{G_\sigma ||g(N_{cd}) - g(N_{ab})||^2}{h^2}} \tag{8}$$

Step 4. Averaging the weighing sum of pixel of intensities and generation of noise-free pixels by using NLM filter.

Let g(a,b) is the input noisy image of size A and the NLM filtered output of the noisy image is defined as Manjón et al. (2008):

$$G(c,d) = \sum_{a=0}^{A-1} \sum_{b=0}^{B-1} W(c,d,a,b) g(a,b) \tag{9}$$

Step 5. Removal of noise bias and obtaining noise free image.

Noise in MRI follows a Rician distribution which results Rayleigh distribution in low intensity region and for higher intensity region results Gaussian distribution. This results the decrease in image contrast. This problem can be overcome by subtracting the noise bias from the square of the MRI magnitude image (Sharma and Chaurasia 2021). So the noise bias can be easily removed from the NLM filtered image as it is signal independent. The unbiased non local mean filter can be found out by Nowak (1999):

$$UNLM[G(c,d)] = \sqrt{G(c,d)^2 - 2\sigma_\eta^2} \tag{10}$$

where $2\sigma_n^2$ =noise bias and σ_n is the standard deviation of the noise and is calculated by using equation (6).

4 Simulation results

In this section we present experimental results to demonstrate the validity of the proposed filter. Firstly, dataset information along with experimental setting is discussed. Next, evaluation metric followed by detail results are also given.

4.1 Dataset and experimental settings

Two kinds of datasets for different noise variances: 0.1, 0.3 and 0.5, are simulated in MATLAB environment.The first kind of dataset is real MR images collected from OSIRIX DICOM (Digital Imaging and Communications in Medicine) image library (Osirix 2014). A total of 100 MRI images were collected and resize to 400 × 400. The second dataset are synthetic images: the self-generated image and the head phantom Image. The generated image with the size (173 × 184), consists of circles and rectangles of various intensities. The head phantom image with the size 256 × 256 was generated in MATLAB environment. Simulation work is performed in MATLAB R2019a environment and the same is used for comparison with existing methods. Wavelet decomposition is performed by using Daubechies 8 (db8), Discrete Wavelet Transform (DWT) and it is preferred due to its orthogonality property (Sahu et al. 2019a, c).

Quantitative comparison is performed through image quality and performance indexes likely Peak Signal to Noise Ratio (PSNR), Correlation of coefficient (COC), Pratt's Figure of Merit (FOM), Mean Structural Similarity Index (MSSIM) and Edge Preservation Index (EPI) (Kanoun et al. 2020; Sahu et al. 2018, 2019a, 2020b). PSNR Measures the quality of reconstructed image and provides the ratio between the original data and the noise introduced. COC determines the interdependence between the reconstructed and original images. FOM measures the dislocated or misplaced edge pixels during reconstruction process. EPI measures the extent of edge preservation in reconstructed image. MSSIM is a quality assessment index that measures the similarity between original and reconstructed images.

4.2 Results and discussion

The ability of the proposed method on removing the noise and preserving the original image properties is proved by comparison with the widely known existing methods, are Unbiased NLM filter (Manjón et al. 2008), KS-NLM method (Rajan et al. 2014), and NLML method (He and Greenshields 2008).The qualitative comparison of the de-noising schemes is performed through visual inspection. Figure 7 shows the visual comparison between the existing and proposed methods. First row shows the simulation results of real Brain MRI. Second row shows the simulation results for real spine MRI. And the third row shows the experimental results of real Sagittal T1 Brain MRI. Better evaluation of filter performance can be done by selecting a small area and applying the filter methods. Figure 8 shows the visual image quality comparison for the small selected area marked as red box. It is seen that the contrast and visual quality of the proposed method is superior to other methods. Qualitative assessment for filtering methods is shown in Fig. 9 for synthetic images. First row shows the simulation result for self-generated synthetic image and the second row shows for head phantom synthetic image.

Proposed method's efficiency on noise removal and edge and details preservation can be confirmed by the performance parameters values. The performance and quality parameters comparison for non-local methods for self-generated synthetic image are discussed in Tables 1, 2, 3, 4 and 5 and for real brain MR image is discussed in Table 6. In

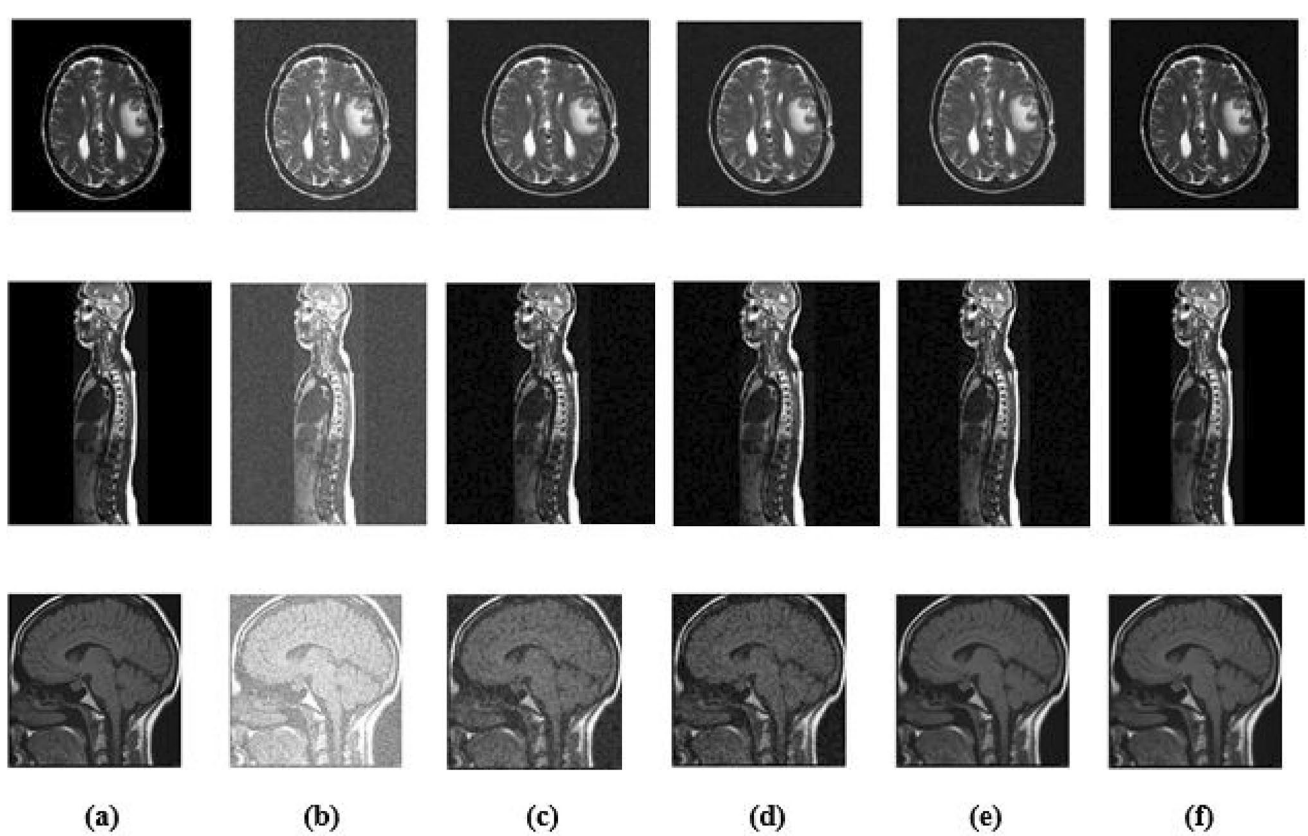

Fig. 7 De-noising Performance result of MR Images (a) Real MR images (b) Degraded by White Gaussian Noise (first row, second row and third row by standard deviations 0.1, 0.3 and 0.5 respectively) (c) NLML (d) KS-NLM (e) UNLM (f) Proposed Method

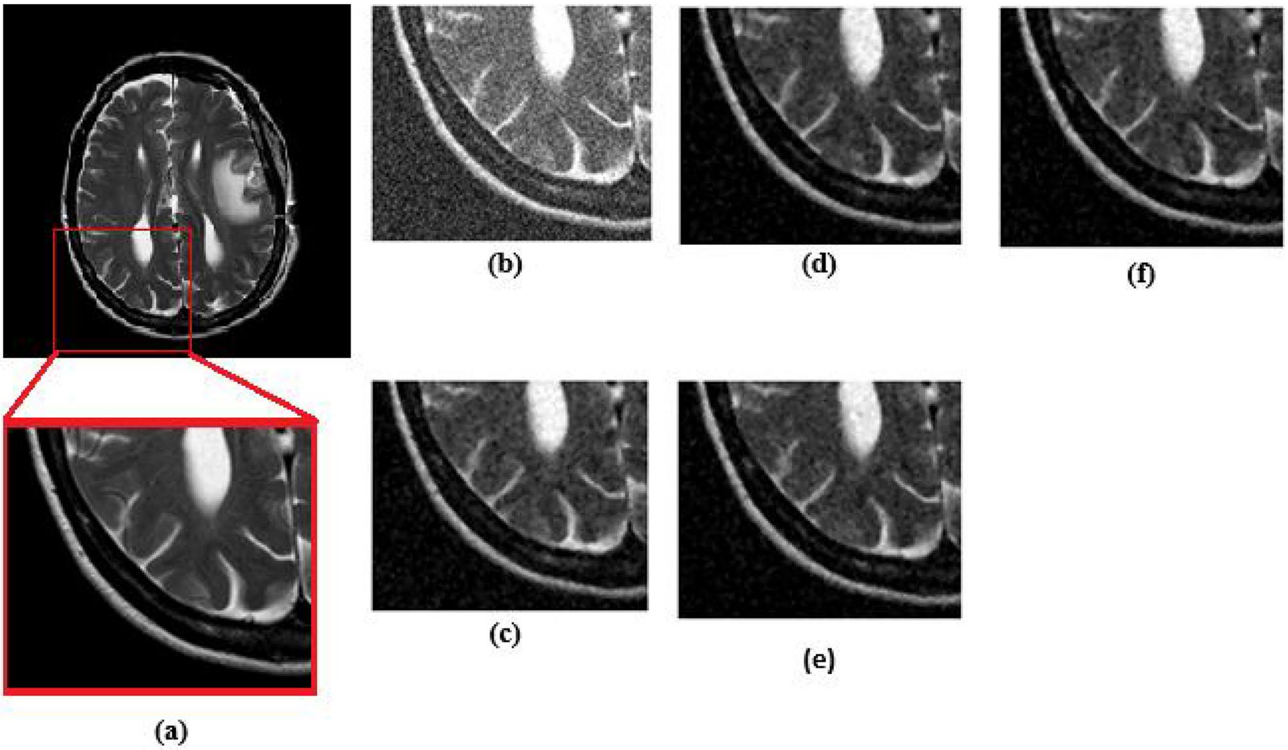

Fig. 8 De-noising performance result of a Zoomed view of a small selected area, **a** real MR image, **b** noisy Image degraded by Gaussian noise of $\sigma_n^2 = 0.3$ **c** NLML **d** KS-NLM **e** UNLM **f** proposed method

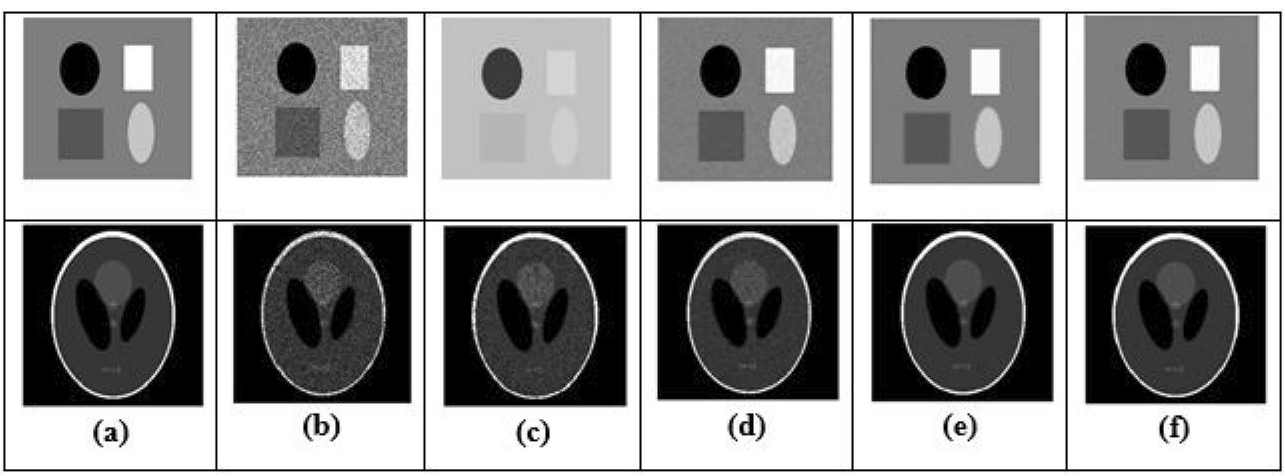

Fig. 9 De-noising performance result of synthetic images **a** original image **b** noisy synthetic Image (Gaussian Noise of $\sigma_n^2 = 0.2$) **c** NLML **d** KS-NLM **e** UNLM **f** proposed method

Table 1, we compare our proposed filter in terms of PSNR with compared methods (Manjón et al. 2008; Rajan et al. 2014) and He and Greenshields (2008) by using synthetic image with three different noise variances. If we set value of $\sigma_n^2 = 0.1$, the PSNR (in dB) score is 33.66. If we set value of $\sigma_n^2 = 0.3$, the PSNR (in dB) score is 32.43. If we set value of $\sigma_n^2 = 0.5$, the PSNR(in dB) score is 30.09. This Table shows that value of PSNR as obtained by our scheme is

Table 1 PSNR (dB) values for different techniques

Techniques	Noise variances		
	0.1	0.3	0.5
Noisy	19.26	14.15	12.59
Unbiased NLM (Manjón et al. 2008)	31.41	30.29	28.25
KS-NLM (Rajan et al. 2014)	30.35	27.68	25.33
NLML (He and Greenshields 2008)	27.89	26.29	22.47
Proposed	33.66	32.43	30.09

always greater than 30.09. The best improvements of our suggested scheme on PSNR score compared with the scheme in Manjón et al. (2008), Rajan et al. (2014) and He and Greenshields (2008) are 6.68% (for $\sigma_n^2 = 0.1$), 15.81% (for $\sigma_n^2 = 0.5$), and 25.32% (for $\sigma_n^2 = 0.5$), respectively. In Table 2, we compare our proposed filter in terms of CoC with compared methods (Manjón et al. 2008; Rajan et al. 2014), and He and Greenshields (2008) by using synthetic image with three different noise variances. If we set value of $\sigma_n^2 = 0.1$, the CoC score is 0.989. If we set value of $\sigma_n^2 = 0.3$, the CoC score is 0.974. If we set value of $\sigma_n^2 = 0.5$, the CoC score is 0.957. This Table shows that value of CoC as obtained by our scheme is always greater than 0.957.The best improvements of our suggested scheme on CoC score compared with the scheme in Manjón et al. (2008), Rajan et al. (2014) and He and Greenshields (2008) are 4.07% (for $\sigma_n^2 = 0.5$), 6.68% (for $\sigma_n^2 = 0.5$), and 11.26% (for $\sigma_n^2 = 0.3$) respectively. In Table 3, we compare our proposed filter in terms of FOM with compared methods (Manjón et al. 2008; Rajan et al. 2014), and He and Greenshields (2008) by using synthetic image with three different noise variances. If we set value of $\sigma_n^2 = 0.1$, the FOM score is 0.968. If we set value of $\sigma_n^2 = 0.3$, the FOM score is 0.953. If we set value of $\sigma_n^2 = 0.5$, the FOM score is 0.89. This Table shows that value of FOM as obtained by our scheme is always greater than 0.953.The best improvements of our suggested scheme on FOM score compared with the scheme in Manjón et al. (2008), Rajan et al. (2014) and He and Greenshields (2008) are 3.88% (for $\sigma_n^2 = 0.3$), 15.61% (for $\sigma_n^2 = 0.5$), and 19.93% (for $\sigma_n^2 = 0.3$), respectively. In Table 4, we compare our proposed filter in terms of MSSIM with compared methods (Manjón et al. 2008; Rajan et al. 2014), and He and Greenshields (2008) by using synthetic image with three different noise variances. If we set value of $\sigma_n^2 = 0.1$, the MSSIM score is 0.877. If we set value of $\sigma_n^2 = 0.3$, the MSSIM score is 0.851. If we set value of $\sigma_n^2 = 0.5$, the MSSIM score is 0.825. This Table shows that value of MSSIM as obtained by our scheme is always greater than 0.825. The best improvements of our suggested scheme on MSSIM score compared with the

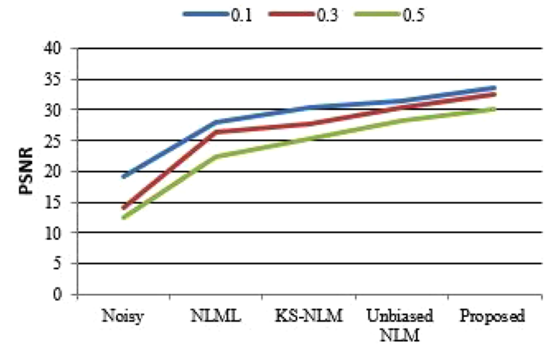

Fig. 10 Graphical comparison of schemes in terms of PSNR

Table 2 CoC results for different techniques

Techniques	Noise variances		
	0.1	0.3	0.5
Noisy	0.823	0.766	0.635
Unbiased NLM (Manjón et al. 2008)	0.971	0.959	0.918
KS-NLM (Rajan et al. 2014)	0.921	0.915	0.893
NLML (He and Greenshields 2008)	0.895	0.866	0.858
Proposed	0.989	0.974	0.957

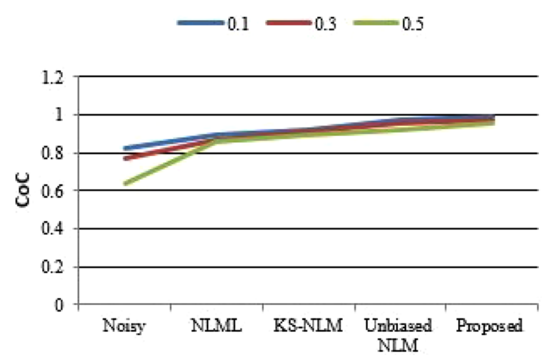

Fig. 11 Graphical comparison of schemes in terms of CoC

Table 3 FOM results for different techniques

Techniques	Noise variances		
	0.1	0.3	0.5
Noisy	0.711	0.623	0.605
Unbiased NLM (Manjón et al. 2008)	0.935	0.916	0.863
KS-NLM (Rajan et al. 2014)	0.850	0.831	0.751
NLML (He and Greenshields 2008)	0.832	0.763	0.720
Proposed	0.968	0.953	0.890

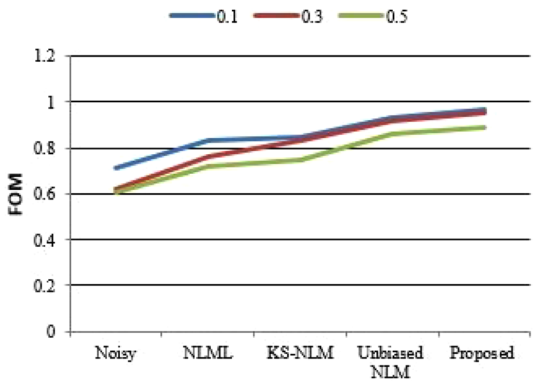

Fig. 12 Graphical comparison of schemes in terms of FOM

Table 4 MSSIM results for different techniques

Techniques	Noise variances		
	0.1	0.3	0.5
Noisy	0.638	0.599	0.454
Unbiased NLM (Manjón et al. 2008)	0.844	0.827	0.809
KS-NLM (Rajan et al. 2014)	0.755	0.728	0.684
NLML (He and Greenshields 2008)	0.735	0.61	0.592
Proposed	0.877	0.851	0.825

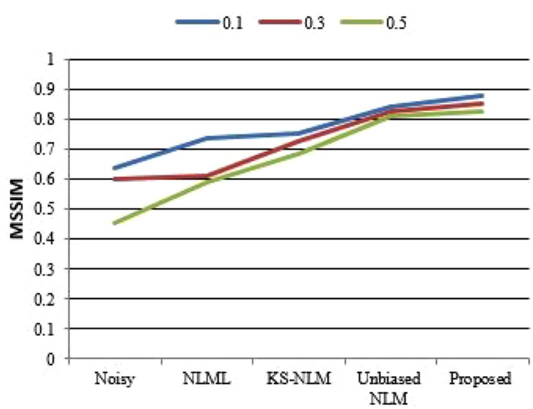

Fig. 13 Graphical comparison of schemes in terms of MSSIM

scheme in Manjón et al. (2008), Rajan et al. (2014) and He and Greenshields (2008) are 3.71% (for $\sigma_n^2 = 0.1$),17.09%(for $\sigma_n^2 = 0.5$), and 28.31%(for $\sigma_n^2 = 0.3$), respectively. In Table 5, we compare our proposed filter in terms of MSSIM with compared methods (Manjón et al. 2008; Rajan et al. 2014), and He and Greenshields (2008) by using synthetic image with three different noise variances. If we set value of $\sigma_n^2 =$ 0.1, the EPI score is 0.788. If we set value of $\sigma_n^2 = 0.3$, the

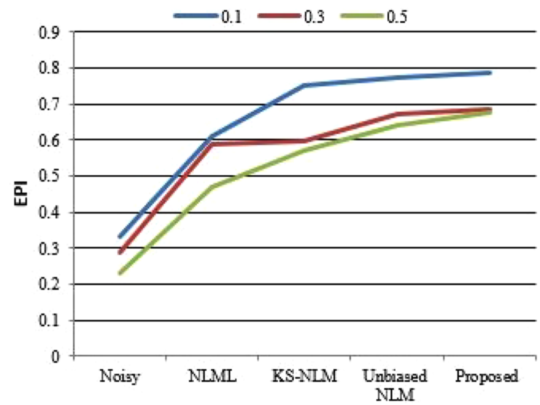

Fig. 14 Graphical comparison of filters in terms of EPI

EPI score is 0.685. If we set value of $\sigma_n^2 = 0.5$, the EPI score is 0.675. This Table shows that value of EPI as obtained by our scheme is always greater than 0.675. The best improvements of our suggested scheme on EPI score compared with the scheme in Manjón et al. (2008), Rajan et al. (2014) and He and Greenshields (2008) are 7.24% (for $\sigma_n^2 = 0.5$), 15.4% (for $\sigma_n^2 = 0.5$), and 30.81% (for $\sigma_n^2 = 0.5$), respectively.

Table 6 shows the comparison of Non Local filters with the proposed filter for real image in terms of the performance parameters. The proposed methodology performed well in terms of edge and structure preservation and noise reduction. The proposed methodology improved 6.35%in terms of PSNR, 2.22% in terms of CoC, 2.91% in terms of FOM, 11.9% in terms of MSSIM and 5.76% in terms of EPI over Unbiased NLM method (Manjón et al. 2008), the next best method. The graphical comparison of performance indexes for all Non Local filters and proposed method for self-generated synthetic image are shown in Figs. 10, 11, 12, 13 and 14, for noise variances 0.1 (Green color), 0.3 (Red color) and 0.5 (Blue color). Performance indexes comparison for real Brain MRI is shown in Fig. 15. All the parameter values are plotted as a function of noise variance. It is seen that the proposed filtering method performs better than the compared schemes.

5 Conclusion

In this paper, we have suggested an improved unbiased-NLM filter to solve the de-noising issue in the MRI images. An unbiased NLM filter is designed by combining the features of NLM filter and the local statistics of the noise.The noise variance is calculated from the complex dataset assuming the noise is distributed in Gaussian nature.Compared

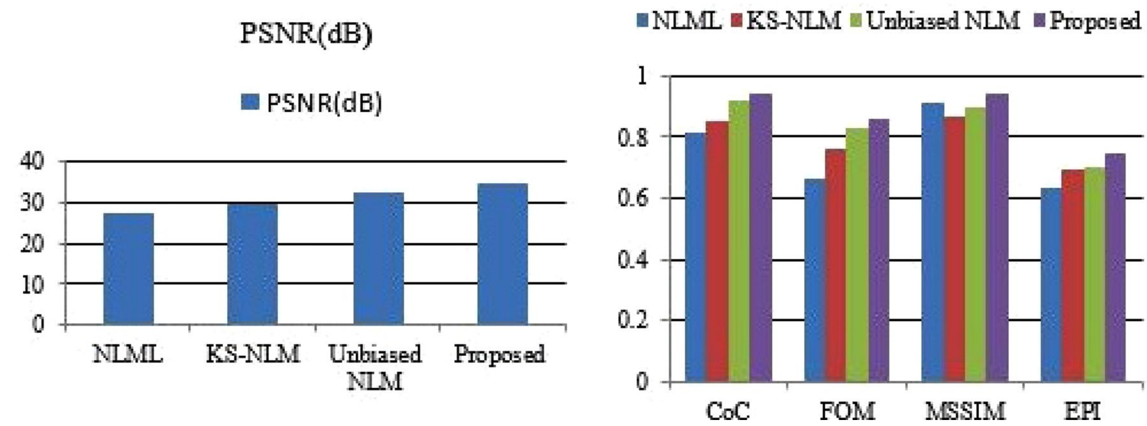

Fig. 15 Graphical comparison of filters in terms of Performance Index for Real brain MR Image

Table 5 EPI results for different techniques

Techniques	Noise variances		
	0.1	0.3	0.5
Noisy	0.334	0.287	0.231
Unbiased NLM (Manjón et al. 2008)	0.775	0.673	0.642
KS-NLM (Rajan et al. 2014)	0.75	0.597	0.571
NLML (He and Greenshields 2008)	0.612	0.589	0.467
Proposed	0.788	0.685	0.675

with the traditional existing non-local mean filtering technology, this proposed filter has the following advantages: (1) Through statistically modeling the wavelet coefficients, accurate noise variance is computed to remove the Gaussian and Rician noise from MR-image (2) By using the accurate estimation of noise bias by statistically modeling the diagonal detail wavelet coefficients, the strength of our proposed de-noising mechanism is further improved.Our experiments on OSIRIX DICOM MRI dataset and some self-generated synthetic images demonstrate that promising results against attacks. Comparison with the non-local mean filtering technology algorithms, the proposed filter has more excellent results.In future the de-noising results may be improved by modeling the wavelet coefficient by Rayleigh distribution to find the Rician noise information.

Table 6 Parameter values for Different Non Local Methods for Real brain MR Image

Techniques	Performance parameters				
	PSNR (dB)	CoC	FOM	MSSIM	EPI
Unbiased NLM (Manjón et al. 2008)	32.56	0.921	0.833	0.901	0.703
KS-NLM (Rajan et al. 2014)	29.69	0.854	0.765	0.866	0.696
NLML (He and Greenshields 2008)	27.38	0.812	0.667	0.911	0.636
Proposed	34.77	0.942	0.858	0.946	0.746

Data availability No data were used to support this study.

References

Anila S, Sivaraju S, Devarajan N (2017) A new contourlet based multiresolution approximation for MRI image noise removal. Natl Acad Sci Lett 40(1):39–41

Bhadauria H, Dewal M (2013) Medical image denoising using adaptive fusion of curvelet transform and total variation. Comput Electric Eng 39(5):1451–1460

Buades A, Coll B, Morel JM (2005) A non-local algorithm for image denoising. In: 2005 IEEE Computer Society Conference on computer vision and pattern recognition (CVPR'05), IEEE, vol 2, pp 60–65

Chen K, Lin X, Hu X, Wang J, Zhong H, Jiang L (2020) An enhanced adaptive non-local means algorithm for Rician noise reduction in magnetic resonance brain images. BMC Med Imaging 20(1):1–9

Das P, Pal C, Chakrabarti A, Acharyya A, Basu S (2020) Adaptive denoising of 3d volumetric MR images using local variance based estimator. Biomed Signal Process Control 59:101901

Gonzalez R, Woods R (2002) Digital image processing, 2nd edn. Prentice Hall, Upper Saddle River

Hamarneh G, Hradsky J (2007) Bilateral filtering of diffusion tensor magnetic resonance images. IEEE Trans Image Process 16(10):2463–2475

Hanchate V, Joshi K (2020a) Denoising of MRI images using fast NLM. J Electric Eng Comput Sci (IJEECS) 18(1):135–141

Hanchate V, Joshi K (2020b) MRI denoising using bm3d equipped with noise invalidation denoising technique and VST for improved contrast. SN Appl Sci 2(2):1–8

He L, Greenshields IR (2008) A nonlocal maximum likelihood estimation method for Rician noise reduction in MR images. IEEE Trans Med Imaging 28(2):165–172

Heo YC, Kim K, Lee Y (2020) Image denoising using non-local means (NLM) approach in magnetic resonance (MR) imaging: a systematic review. Appl Sci 10(20):7028

Hong D, Huang C, Yang C, Li J, Qian Y, Cai C (2020) FFA-DMRI: a network based on feature fusion and attention mechanism for brain MRI denoising. Front Neurosci 14:934

Kagoiya K, Mwangi E (2017) A hybrid and adaptive non-local means wavelet based MRI denoising method with bilateral filter enhancement. Int J Comput Appl 166:1–7

Kanoun B, Ambrosanio M, Baselice F, Ferraioli G, Pascazio V, Gómez L (2020) Anisotropic weighted KS-NLM filter for noise reduction in MRI. IEEE Access 8:184866–184884

Kollem S, Rama Linga Reddy K, Srinivasa Rao D (2020) Modified transform-based gamma correction for MRI tumor image denoising and segmentation by optimized Histon-based elephant herding algorithm. Int J Imaging Syst Technol 30(4):1271–1293

Krissian K, Aja-Fernández S (2009) Noise-driven anisotropic diffusion filtering of MRI. IEEE Trans Image Process 18(10):2265–2274

Leal N, Zurek E, Leal E (2020) Non-local SVD denoising of MRI based on sparse representations. Sensors 20(5):1536

Macovski A (1996) Noise in MRI. Magn Reson Med 36(3):494–497

Manjon J, Robles M, Thacker N (2007) Multispectral MRI de-noising using non-local means. Med Image Underst Anal (MIUA), pp 41–46

Manjón JV, Carbonell-Caballero J, Lull JJ, García-Martí G, Martí-Bonmatí L, Robles M (2008) MRI denoising using non-local means. Med Image Anal 12(4):514–523

McVeigh E, Henkelman R, Bronskill M (1985) Noise and filtration in magnetic resonance imaging. Med Phys 12(5):586–591

Nowak RD (1999) Wavelet-based Rician noise removal for magnetic resonance imaging. IEEE Trans Image Process 8(10):1408–1419

Osirix (2014) Osirix dicom image. http://www.osirix-viewercom/resources/diacom-image-library/. Accessed 13 Mar 2021

Rajan J, Arnold J, Sijbers J (2014) A new non-local maximum likelihood estimation method for Rician noise reduction in magnetic resonance images using the Kolmogorov-Smirnov test. Signal Process 103:16–23

Redpath TW (1998) Signal-to-noise ratio in MRI. Br J Radiol 71(847):704–707

Richardson JC, Bowtell RW, Mäder K, Melia CD (2005) Pharmaceutical applications of magnetic resonance imaging (MRI). Adv Drug Deliv Rev 57(8):1191–1209

Romdhane F, Villano D, Irrera P, Consolino L, Longo DL (2021) Evaluation of a similarity anisotropic diffusion denoising approach for improving in vivo CEST-MRI tumor pH imaging. Magn Reson Med 85(6):3479–3496

Sahu S, Singh HV, Kumar B, Singh A (2018) Statistical modeling and Gaussianization procedure based de-speckling algorithm for retinal oct images. J Ambient Intell Human Comput. https://doi.org/10.1007/s12652-018-0823-2

Sahu S, Singh HV, Kumar B, Singh AK (2019a) De-noising of ultrasound image using Bayesian approached heavy-tailed Cauchy distribution. Multimed Tools Appl 78(4):4089–4106

Sahu S, Singh HV, Kumar B, Singh AK, Kumar P (2019b) Enhancement and de-noising of oct image by adaptive wavelet thresholding method. In: Singh AK, Mohan A (eds) Handbook of multimedia information security: techniques and applications. Springer, pp 449–471

Sahu S, Singh HV, Kumar B, Singh AK, Kumar P (2019c) Image processing based automated glaucoma detection techniques and role of de-noising: a technical survey. In: Singh AK, Mohan A (eds) Handbook of multimedia information security: techniques and applications. Springer, pp 359–375

Sahu S, Singh HV, Kumar B, Singh AK (2020a) A Bayesian multiresolution approach for noise removal in medical magnetic resonance images. J Intell Syst 29(1):189–201

Sahu S, Singh HV, Singh AK, Kumar B (2020b) Mr image denoising using adaptive wavelet soft thresholding. In: Dutta D, Kar H, Kumar C, Bhadauria V (eds) Advances in VLSI, communication, and signal processing. Springer, pp 775–785

Sarkar S, Tripathi PC, Bag S (2020) An improved non-local means denoising technique for brain MRI. In: Das AK, Nayak J, Naik B, Pati SK, Pelusi D (eds) Computational intelligence in pattern recognition. Springer, pp 765–773

Sharma A, Chaurasia V (2021) Mri denoising using advanced NLM filtering with non-subsampled Shearlet transform. Signal Image Video Process 15:1–9

Sijbers J, den Dekker AJ, Van Audekerke J, Verhoye M, Van Dyck D (1998) Estimation of the noise in magnitude MR images. Magn Reson Imaging 16(1):87–90

Upadhyay P, Upadhyay S, Shukla K (2021) Magnetic resonance images denoising using a wavelet solution to Laplace equation associated with a new variational model. Appl Math Comput 400:126083

Xie D, Li Y, Yang H, Bai L, Wang T, Zhou F, Zhang L, Wang Z (2020) Denoising arterial spin labeling perfusion MRI with deep machine learning. Magn Reson Imaging 68:95–105

Zhu H, Li Y, Ibrahim JG, Shi X, An H, Chen Y, Gao W, Lin W, Rowe DB, Peterson BS (2009) Regression models for identifying noise sources in magnetic resonance images. J Am Stat Assoc 104(486):623–637